Green Grant-Free Power Allocation for Ultra-Dense Internet of Things: A Mean-Field Perspective★

Sami Nadif[a], Essaid Sabir[b,*], Halima Elbiaze[c] and Abdelkrim Haqiq[a]

[a]Computer Networks, Mobility and Modeling Laboratory (IR2M), FST, Hassan I University of Settat, 26000, Morocco
[b]Department of Science and Technology, TÉLUQ, University of Quebec, Montreal, H2S 3L4, Quebec, Canada
[b]Department of Computer Science, University of Quebec at Montreal (UQAM), Montreal, H2L 2C4, Quebec, Canada

ARTICLE INFO

Keywords:
Internet of Things (IoT)
Grant-Free Access
Massive IoT
Ultra-Dense Networks
Power Allocation
Mean-Field Game

ABSTRACT

Grant-free access, in which each Internet-of-Things (IoT) device delivers its packets through a randomly selected resource without spending time on handshaking procedures, is a promising solution for supporting the massive connectivity required for IoT systems. In this paper, we explore grant-free access with multi-packet reception capabilities, with an emphasis on ultra-low-end IoT applications with small data sizes, sporadic activity, and energy usage constraints. We propose a power allocation scheme aimed at maximizing throughput while minimizing power consumption by considering the traffic and energy constraints of IoT devices. Our approach employs a stochastic geometry framework and mean-field game theory to model and analyze the mutual interference among active IoT devices. Additionally, we utilize a Markov chain model to capture and track the queue length of IoT devices, enabling the derivation of the transmission success probability at steady-state. The simulation results illustrate the optimal power allocation strategy and evaluate the proposed approach's performance in terms of packet transmission success probability and average delay.

1. Introduction

Massive Internet of Things (IoT) communications are essential in the fifth-generation (5G) and beyond cellular networks [1, 2, 3, 4]. They are distinguished by a large number of low-cost IoT devices that operate mostly in the uplink and have small packets, sporadic activity, and restrictive energy usage requirements. Hence, massive IoT requires a whole different set of Medium Access Control (MAC) protocols than those intended for human-centric communications. To be more specific, existing cellular networks use Grant-Based (GB) transmission, which means that each IoT device must conduct a handshake procedure to establish a connection with the Base Station (BS) anytime a new packet needs to be sent. Furthermore, the handshake procedure involves exchanging multiple signaling messages (i.e., scheduling request, scheduling grant, and resource allocation) to facilitate exclusive channel access, which might take several tens of milliseconds [5]. However, as packet sizes shrink and the number of IoT devices grows, this handshake procedure becomes inefficient, potentially resulting in overhead signaling and radio access congestion [6]. Additionally, the number of signaling messages has a significant impact on the energy efficiency of IoT devices (shorter transmissions preserve energy). To address these issues, Grant-Free (GF) transmission [5, 7, 8, 9] is a promising solution. This approach removes the need for a handshaking process by allowing each IoT device to send its packets across a randomly selected resource without prior coordination with the BS. SigFox and LoRa are two examples of low-power wide-area network technologies that implement GF transmission for efficient IoT connectivity [10, 11]. This is made possible through the use of low-complexity contention-based random access schemes, such as variations of the well-known ALOHA protocol [12, 13], making GF transmission ideal for large-scale IoT networks with infrequent communication needs. However, since the orthogonal resources are not allocated by the base station, numerous IoT devices may use the same resource for transmission, potentially resulting in a collision. To reduce the effects of collisions, non-orthogonal

★A preliminary version of this article has been presented at the 20th Mediterranean Communication and Computer Networking Conference (MedComNet 2022).

*Corresponding author
s.nadif@uhp.ac.ma (S. Nadif); essaid.sabir@teluq.ca (E. Sabir); elbiaze.halima@uqam.ca (H. Elbiaze); abdelkrim.haqiq@uhp.ac.ma (A. Haqiq)
ORCID(s): 0000-0003-4141-5491 (S. Nadif); 0000-0001-9946-5761 (E. Sabir); 0000-0001-5681-6445 (H. Elbiaze); 0000-0002-8857-6586 (A. Haqiq)

multiple access protocols can be used in conjunction with random access schemes [5, 14]. More specifically, the Multi-Packet Reception (MPR) capability [15, 16] given by a non-orthogonal transmission mechanism enables numerous IoT devices to use the same resource and transmit their packets concurrently, reducing the occurrence of packet collisions. Nevertheless, the performance of grant-free access with MPR capability degrades in a massive IoT environment with sporadic traffic [17]. Thus, in order to take full advantage of this solution, a distributed resource management technique such as power control [18, 19, 20] must be considered. Power control was originally employed in cellular networks to manage interference, but it is also a flexible mechanism to provide quality of service and reduce energy consumption. Thus, grant-free transmission, when combined with an effective power allocation strategy, can therefore meet the 5G standards for IoT devices, which include a battery life of more than ten years [21].

In this paper, we consider large-scale ultra-dense IoT networks using grant-free transmission with J-MPR capability (assuming that up to J collided IoT devices can be decoded on a single resource), and we focus on ultra-low-end IoT applications with small data sizes, sporadic activity, and restrictive energy usage requirements. We construct an analytical model that considers both spatial randomness and temporal traffic generation. For the tractability of our analysis, both BSs and IoT devices are modeled using a homogeneous Poisson Point Process (PPP), where the BSs boundaries can be shown by a weighted Voronoi tessellation. Stochastic geometry, particularly point process theory, is widely used to model the spatial topology of cellular networks, and several empirical foundations validate the PPP model [22, 23]. It is noteworthy that, in practical scenarios, achieving a high level of positioning accuracy is possible [24]. This aspect is particularly significant as it enhances the precision of location information in real-world applications.
From a temporal perspective, our model addresses sporadic IoT traffic, where packet arrivals at each IoT device follow a Bernoulli process with a small arrival rate. The main difficulty in considering a spatiotemporal model is that the set of active IoT devices that cause interference changes dramatically over time. Thus, to assess the uplink performance of the grant-free transmission in a massive IoT network, manage inter-cell interference, and avoid unnecessary energy wastage, we propose a distributed uplink power allocation strategy under spatiotemporal fluctuation. The power allocation problem is initially treated as a differential game due to the coupling in interference. Then, by using the stochastic geometry framework and Mean-Field Game (MFG) theory to model and analyze mutual interference among active IoT devices, we extend the differential game to a MFG. The MFG framework enables each IoT device to determine its optimal power allocation strategy based on its own energy budget and the statistical distribution of the system state, known as the mean-field. Moreover, we develop a Markov chain model to monitor the IoT device's queue length and derive the steady-state transmission success probability. Finally, by formulating the problem as a mean-field optimal control problem, we can obtain a set of equations that allow us to achieve the mean-field equilibrium through an iterative solution.

1.1. Related Work

The use of game theory in the analysis of random access schemes has been widely studied over the past decades [25, 26, 27, 28]. Game theory provides a way to analyze the decision-making process between multiple individuals or entities who are interacting with each other, and it has been used to study various aspects of random access schemes, such as user behavior and system performance optimization. The authors in [25], for example, use game theory to analyze the Aloha protocol from the perspective of selfish users who have two possible actions: transmit or wait. The authors construct an Aloha game to study the optimal behavior of individual users and show that the Aloha game has an equilibrium. The authors in [26] analyze the ALOHA protocol with users having two transmission power levels and use two non-cooperative optimization concepts, the Nash equilibrium and the evolutionary stable strategy. The performance of these concepts is compared with a cooperative solution and the impact of multiple power levels is analyzed. Game theory has also been used to capture the interactions between a set of IoT devices and predict their optimal strategies on contemporary IoT networks by analyzing the Nash and/or Stackelberg equilibrium [29]. The authors in [30] use the Nash equilibrium to provide an energy-efficient access point allocation in an IoT network. In [31], the authors use the age of information metric to analyze the competition between multiple IoT devices, who can choose their own transmission probability, in an irregular repetition slotted Aloha IoT system. By analyzing the Nash equilibrium, they highlight that introducing a transmission cost can regulate the overall performance. In contrast, related works based on

the Stackelberg equilibrium concept include [32, 33], which develop and analyze hierarchical game models for IoT networks based on the leader/follower principle. The authors in [32], for example, develop a multi-leader/multi-follower Stackelberg game to provide a caching strategy in a 5G-enabled IoT network by analyzing a competitive scenario with various 5G mobile network operators and different content providers.
However, when dealing with a large number of IoT devices, the atomic equilibrium concepts become extremely challenging. In this circumstance, it is more interesting for an IoT device to deal with collective behavior than with the specific individual strategy of each IoT device. Hence, the Mean-Field Game (MFG) theory [34, 35, 36, 37, 38] has increasingly gained attention in massive IoT networks. Related works analyzing the mean-field equilibrium in massive IoT networks could be found in [39, 40, 41, 42]. For example, the authors in [40] investigate delay-optimal random access in large-scale energy harvesting IoT networks. They handle the coupling between the data and energy queues using a two-dimensional Markov decision process, and they employ the MFG theory to disclose the coupling among IoT devices by exploiting the large-scale property. In [42], under the grant-free communication framework, the age of information minimization problem is analyzed in a massive IoT network using a mean-field evolutionary game-based approach by optimizing packet sampling and scheduling.

The works related to grant-free transmission, on the other hand, include [8], where a Semi-Granted Multiple Access (SGMA) approach is analyzed for non-orthogonal multiple access in 5G networks, allowing grant-based and grant-free transmission to share the same wireless resource. Then, a heuristic SGMA resource allocation algorithm is presented to enhance network capacity and user connectivity. The authors in [43] present a grant-free user activity detection scheme in a massive IoT network with extremely low complexity and latency. They use multiple antennas at the base station to generate spatial filtering via a fixed beamforming network, which reduces inter-beam interference. They also suggest using orthogonal multiple access technology to minimize intra-beam interference in the temporal domain. In [7], the authors investigate an asynchronous grant-free transmission protocol with the goal of reducing energy consumption and delay by relaxing the synchronization requirement at the cost of sending multiple packet replicas and using a more complex signal processing technique. The suggested approach is scrutinized by developing closed-form expressions for critical performance characteristics, including reliability and battery life. Related works that investigate spatiotemporal modeling [44, 45] for grant-free transmission can be found in [46, 47]. The authors in [46] analyze three grant-free transmission schemes that use Hybrid Automatic Repeat reQuest (HARQ) retransmissions: reactive, K-repetition, and proactive. They provide a spatiotemporal assessment model for contention-based grant-free transmission and define the access failure probability to evaluate the reliability and latency performance under the three grant-free HARQ schemes. In [47], the authors investigate the energy efficiency and packet transmission probability in grant-free uplink IoT networks. To do this, a spatiotemporal model is constructed leveraging queueing theory and a stochastic geometry framework, where each device is represented by a two-dimensional discrete-time Markov chain and expected to use full path loss inversion power control with a target power level. In a similar vein, our work also examines grant-free transmission using a spatiotemporal model. However, instead of relying on path loss inversion power control, we employ a power allocation strategy based on mean-field game theory. Within this framework, we also aim to analyze energy efficiency and packet transmission probability.

1.2. Our Contributions

The contributions of this paper are manifold and can be summarized as follows:

(1) We present a spatiotemporal model for grant-free transmission with J-MPR capability by using stochastic geometry and Markov chain theory. From a spatial perspective, stochastic geometry is applied to model and analyze the mutual interference among active IoT devices (i.e., those with at least one packet in their queue). From a temporal perspective, Markov chain theory is used to model the correlation of the number of packets in a queue over different frames.

(2) To address the issue of the large number of IoT devices, we present a mean-field power allocation scheme that integrates the IoT device's traffic generation and energy budget. Our approach enables IoT devices to distributively compute their power allocation control strategies without having complete awareness of the strategies or states of other IoT devices.

(3) We combine stochastic geometry analysis and mean field formulation to derive the transmission success probability in a massive grant-free IoT network (see proposition 2). The success probability in the paper's model is influenced by multiple factors, such as IoT density, arrival rate, base station density, and multi-packet reception capability.

(4) We assess the performance of a massive grant-free IoT network with MPR capability in terms of packet transmission success probability and average delay.

The rest of the paper is organized as follows: The section 2 presents the system model and the assumptions. The power allocation problem is formalized in section 3. The section 4 introduces the discrete-time Markov chain model. The section 5 provides the numerical and simulation results. Finally, concluding remarks are given in section 6.

2. System Model

We consider a massive IoT network using an orthogonal multiple access scheme, with the total bandwidth partitioned into L orthogonal channels represented as $\mathbf{L} = \{\ell_i, i = 1, \dots, L\}$. We assume that the total bandwidth is reused throughout the network with a frequency reuse factor of 1. This signifies that each cell has access to the entire set of orthogonal channels, and there is no restriction on the reuse of frequencies across different cells, leading to inter-cell interference. Furthermore, we consider a single-tier of base stations (BS) with Multi-Packet Reception (MPR) capability that are spatially distributed according to a homogeneous PPP denoted by $\phi_s = \{\mathbf{s}_i, i = 1, 2, \dots\}$ with intensity λ_s, where $\mathbf{s}_i$ is the location of the i^{th} BS. We consider a J-MPR model where up to J IoT devices can be decoded on a single channel. We assume that if j IoT devices choose the same channel, there is no packet collision whenever $j \leq J$, whereas all the j IoT devices are not decoded (collided) whenever $j > J$. The IoT devices, on the other hand, are randomly distributed and modeled by a homogeneous PPP denoted by $\phi_u = \{\mathbf{u}_i, i = 1, 2, \dots\}$ with intensity λ_u, where $\mathbf{u}_i$ is the location of the i^{th} IoT device. Each IoT device is served via its geographically nearest BS. Thus, the BS boundaries can be shown by a weighted Voronoi tessellation. An important random parameter is the distance r separating an IoT device from its serving BS. Since each IoT device communicates with the closest BS, no other base station can be closer than r. Thus, the distance of an arbitrary IoT device from its serving BS has a cumulative distribution function given as follows:

$$\begin{aligned} F_r(r_0) &= \mathbb{P}[r \leq r_0] \\ &= 1 - \mathbb{P}[\text{No BS closer than } r_0] \\ &= 1 - e^{-\lambda_s \pi r_0^2}. \end{aligned} \tag{1}$$

Thus, the probability density function can be found as

$$f_r(r) = \frac{dF_r(r)}{dr} = 2\pi\lambda_s r e^{-\lambda_s \pi r^2}. \tag{2}$$

Let V be the area of a Voronoi cell. The number of IoT devices associated with a specific BS of area $V = v$, defined as N_v, follows a Poisson distribution with the probability mass function given by:

$$\mathbb{P}[N_v = k | V = v] = \frac{(\lambda_u v)^k}{k!} e^{-\lambda_u v}, \quad k = 0, 1, \dots \tag{3}$$

Moreover, the Voronoi cell area V is a random variable that can be approximated by the gamma distribution with shape $c = 3.575$ and rate $\lambda_s c$ [48]. The corresponding probability density function is:

$$f_V(v) = \frac{v^{c-1}(\lambda_s c)^c}{\Gamma(c)} e^{-(\lambda_s c)v}, \quad v > 0. \tag{4}$$

From the temporal perspective, we assume that the network operates in a synchronized manner and that the timeline is segmented into frames with duration T_f. This simplifies the user detection procedure since multiple packets are allowed to be sent on the same channel simultaneously. We also assume that the IoT devices use grant-free transmission. In other words, the packet for each IoT device will be transmitted immediately once it is generated. In this paper, the packet arrival process at each IoT device is modeled by a Bernoulli process, which is commonly utilized in discrete-time system modeling, with a small arrival rate $0 \leq p_a \leq 1$ (sporadic activity). Note that p_a is also the probability that an IoT device will generate a packet in a particular frame. Furthermore, IoT devices with a non-empty queue may employ a frame for a single packet uplink transmission attempt. As a result, in each frame, only one packet may arrive and/or depart from the queue of each IoT device in the network. Each IoT device transmits packets via a first-come, first-served packet scheduling scheme and has a queue that can store a maximum of M packets. We also assume that the generated packet is sufficiently small and thus can be successfully transmitted through each transmission attempt if there is no packet collision and the received Signal to Interference-plus-Noise Ratio (SINR) is greater than a threshold θ. Furthermore, we presume that BS employs access barring to control overall traffic load in the system, where IoT devices with at least one packet in their queue, referred to as active IoT devices, attempt uplink transmissions in the current frame with probability $1 - p_b$ or skip it with probability p_b.

In this work, we denote by π_a the probability that an IoT device is active, for which we will derive a closed-form expression in section 4. The active IoT devices that attempt uplink transmissions in a given frame using channel $\ell_i \in \mathbf{L}$ constitute a PPP, denoted by $\phi_a = \{\mathbf{a}_i, i = 1, 2, \dots\}$, with intensity $\lambda_a = ((1-p_b)\pi_a/L)\lambda_u$. Let's N_a be the number of active IoT devices in a given Voronoi cell using channel $\ell_i \in \mathbf{L}$. Therefore, by using (3) and (4), the unconditional probability mass function of N_a, for $k = 0, 1, 2, \dots$, writes

$$\begin{aligned}\mathbb{P}[N_a = k] &= \int_0^\infty \frac{\left(\lambda_a v\right)^k}{k!} e^{-\lambda_a v} f_V(v)\, dv \\ &= \frac{\Gamma(k+c)}{\Gamma(k+1)\Gamma(c)} \cdot \frac{\left(\lambda_a\right)^k (\lambda_s c)^c}{\left(\lambda_a + c\lambda_s\right)^{k+c}}.\end{aligned} \tag{5}$$

In the rest of this paper, we consider a large circle of radius R to be the spatial domain of our analysis, denoted as C_R. It is worth noting that the number of active IoT devices attempting an uplink transmission in a given frame using channel ℓ_i in C_R, denoted as $\mathcal{N}_R$, is a Poisson random variable with a mean intensity $\lambda_a \pi R^2$.

The outcome of a transmission is assessed through the received time-varying SINR. Without loss of generality, the experienced SINR under a Gaussian single-input, single-output channel writes:

$$\Gamma_i(t, P_i, \mathbf{P}_{-i}) = \frac{P_i(t) H_{i,i}(t) D_{i,i}(r)}{\sigma_0 + I_i(t, \mathbf{P}_{-i})}, \tag{6}$$

where in the above expression, $P_i \in [0, P_{max}]$ is the transmit power of IoT device i, $\mathbf{P}_{-i}$ denotes the transmit power vector of the active IoT devices using the same channel without i, $H_{i,j}$ (resp. $D_{i,j}$) is a parameter representing the multipath fading (resp. path-loss) between the IoT device j and BS serving the IoT device i, σ_0 is the noise power, and $I_i(t, \mathbf{P}_{-i})$ denotes the interference caused by the active IoT devices using the same channel for transmission expressed as:

$$I_i(t, \mathbf{P}_{-i}) = \sum_{j=1, j\neq i}^{|\mathcal{N}_R|} P_j(t) H_{i,j}(t) D_{i,j}(r). \tag{7}$$

Finally, we assume that the channel between all the transmitters and all the receivers experiences an independent Rayleigh fading H, exponentially distributed with unity mean, and a path-loss $D(r) = r^{-\alpha}$ with exponent $\alpha > 2$.

3. Power Allocation: A Mean-Field Approach

The MFG stands out as a robust framework for modeling and analyzing large-scale ultra-dense networks, particularly in the context of massive IoT deployments. Specifically, when dealing with a large number of IoT devices, the mean-field approach is more practical than traditional atomic equilibrium concepts, emphasizing collective behavior over specific individual strategies. In this section, we initially approach the power allocation problem as a differential game and subsequently extend it to MFG.

3.1. Differential Game Model

The differential power allocation game is played over time $t \in [0, T_f]$, where T_f represents the frame duration.

- **Player sets:** $\mathcal{N}_R = \{1, 2, \dots, |\mathcal{N}_R|\}$, the active IoT devices that attempt uplink transmissions in a given frame using channel $\ell_i \in \mathbf{L}$
- **State:** The state of an IoT device i time t is described by its remaining energy at that time, given by $E_i(t) \in [0, E_{i,max}]$, evolving according to the following differential equation:

$$d E_i(t) = -P_i(t)\, dt, \tag{8}$$

where $P_i(t)$ is the transmit power, and $E_{i,max} = E_i(0)$ is the energy budget fixed by the IoT device i to spend over $[0, T_f]$. The dynamics (8) implies that the variation in the energy budget during dt is proportional to the transmission power.

- **Actions:** Transmit power $P_i(t) \in [0, P_{max}]$, which is allowed to depend not only on time but also on the state $E_i(t)$ and on the states of all other active IoT devices in the system at time t, denoted as $\mathbf{E}_{-i}(t)$. A power allocation strategy of the IoT device i will be denoted by P_i with $P_i(t) = P_i(t, E_i(t), \mathbf{E}_{-i}(t))$.
- **Utility function:** The goal of each IoT device is to adapt its actions according to its remaining energy while maximizing its throughput. Thus, the average utility function of the IoT device i is given by:

$$U_i(P_i, \mathbf{P}_{-i}, p_s) = \mathbb{E}\left[\int_0^{T_f} F_i(t, P_i, \mathbf{P}_{-i}, p_s)\, dt\right], \tag{9}$$

where

$$F_i := (1 - p_s)P_i - p_s \log_2(1 + \Gamma_i), \tag{10}$$

and p_s is the transmission success probability (see proposition 2).
Such utility function is especially relevant when IoT devices have to trade-off between achieving the highest possible throughput and expending as little power as necessary.
• **Nash equilibrium:** A power allocation strategy profile $\mathbf{P}^* = (P_1^*, P_2^*, \dots, P_{|\mathcal{N}_R|}^*)$ is a feedback Nash equilibrium of the dynamic differential game if and only if $\forall i$, P_i^* is a solution of the following optimal control problem:

$$\inf_{P_i} U_i(P_i, \mathbf{P}_{-i}^*, p_s), \tag{11}$$

subject to

$$d\begin{bmatrix} E_i(t) \\ \mathbf{E}_{-i}(t) \end{bmatrix} = \begin{bmatrix} -P_i(t) \\ -\mathbf{P}_{-i}^*(t) \end{bmatrix} dt, \tag{12}$$

To obtain the optimal power allocation strategies, the standard solution concept consists of analyzing the Nash equilibrium. However, the complexity of this approach increases with the number of IoT devices. Furthermore, it necessitates that each IoT device be fully aware of the states and actions of all other IoT devices, resulting in a tremendous volume of information flow. This is not feasible and impractical for a grant-free, massive IoT network. Nevertheless, since the effect of other IoT devices on a single IoT device's average utility function is only via interference, it is intuitive that, as the number of IoT devices increases, a single IoT device has a negligible effect. Thus, we suggest using a mean-field limit for this game to convert these multiple interactions (interference) into a single aggregate interaction known as mean-field interference. However, the mean-field limit is only significant if the associated approximation error is small. It has been shown that, under appropriate conditions, the mean-field limit realizes an ϵ-Nash equilibrium for the dynamic differential game, with ϵ converging to zero as the number of players goes to infinity [38, 49]. Therefore, in this paper, we consider a large-scale ($R \to \infty$) massive IoT network under the assumption of frequency reuse factor of 1 to assure a small approximation error at the mean-field limit. It is important to note that if the frequency resources are not reused, increasing the number of BS in the network would decrease the number of IoT devices using the same channel for transmission, which would negatively affect the accuracy of the mean-field limit.

3.2. Mean-Field Regime

The general setting of a mean-field regime is based on the following assumptions:
- The existence of large number of IoT devices ensured by considering large-scale, massive IoT network.
- Interchangeability: the permutation of the state (energy budget) among the IoT devices would not affect the optimal power allocation strategy. To guarantee this property, we assume that each IoT device only knows its individual energy budget and implements a homogeneous transmit power $P_i(t) = P(t, E_i(t))$.
- Finite mean-field interference I_{mf} (see proposition 1).

Let $[0, E_{max}]$ be the energy domain of our analysis. We define the empirical energy distribution of the IoT devices in C_R at time t in $[0, T_f]$ as:

$$M(t,e) = \frac{1}{|\mathcal{N}_R|} \sum_{i=1}^{|\mathcal{N}_R|} \delta_e(E_i(t)), \quad \forall e \in [0, E_{max}], \tag{13}$$

where δ_e is the Dirac measure.
The basic idea behind the mean-field regime is to approximate a finite population with an infinite one, where the empirical energy distribution $M(t,e)$ almost surely converges, as $|\mathcal{N}_R| \to \infty$, to the probability density function $m(t,e)$ of a single IoT device, due to the strong law of large numbers. We will refer to the energy distribution $(m_t)_{t\geq 0}$ as the mean-field. Additionally, as the IoT devices become essentially indistinguishable, we can focus on a generic IoT device by dropping its index i where its individual dynamic is written as:

$$\begin{cases} dE(t) = -P\big(t, E(t)\big)\, dt, \quad t \geq 0, \\ E(0) = E_0. \end{cases} \tag{14}$$

Thus, the evolution of the mean-field $(m_t)_{t\geq 0}$ over time t in $[0, T_f]$ is described by a first-order partial differential equation, known as the Fokker-Planck Kolmogorov (FPK) equation, given by [41]:

$$\begin{cases} \partial_t m(t,e) - \partial_e\big(P(t,e)m(t,e)\big) = 0, \\ m(0,.) = m_0. \end{cases} \tag{15}$$

The mean-field regime describes the mass behaviors of IoT devices in a massive IoT network, allowing the generic IoT device to determine its optimal power allocation strategy based only on its own energy budget and the initial mean-field. By expressing the interference in terms of an expectation over the mean-field that changes with time according to the FPK equation, we achieve a remarkable degree of economy in the description of population dynamics.

Proposition 1. *By following a stochastic geometry-based approach, the mean-field interference in a large-scale network for a generic IoT device is derived for $t \in [0, T_f]$ as follows:*

$$I_{mf}(t, \pi_a) = 2\pi\lambda_u \frac{(1-p_b)\pi_a}{L}\left[\frac{1}{2} + \frac{1}{\alpha - 2}\right] P_{mf}(t), \tag{16}$$

where

$$P_{mf}(t) = \int_0^{E_{max}} P(t,e)m(t,e)\,de. \tag{17}$$

Proof. The proof is given in Appendix A.1.

Now, we turn our attention to determining the SINR and the utility function, which are solely dependent on a generic IoT device's individual transmit power and the mean-field. The new parameters of the game are defined as:

• Mean-field SINR: Since the distance of a generic IoT device from its serving BS has a probability density function given by (2) with mean $1/(2\sqrt{\lambda_s})$, we define the mean-field SINR as:

$$\Gamma_{mf}(P, I_{mf}) = \frac{P(t,E)(2\sqrt{\lambda_s})^\alpha}{\sigma_0 + I_{mf}(t,\pi_a)}. \tag{18}$$

• Mean-field utility function: The mean-field utility functions for a generic IoT device is generalized as follows:

$$U_{mf}(P, I_{mf}, p_s) = \int_0^{E_{max}}\int_0^{T_f} F_{mf}(P, I_{mf}, p_s)m(t,e)\,dt\,de, \tag{19}$$

where

$$F_{mf} := (1-p_s)P - p_s\log_2(1+\Gamma_{mf}). \tag{20}$$

3.3. Mean-Field Optimal Control

The mean-field optimal control problem of a generic IoT device is derived based on (11) and consists in finding the optimal power allocation strategy P^* and the mean-field at equilibrium m^* satisfying:

$$\inf_P U_{mf}(P, I^*_{mf}, p_s) \tag{21}$$

where I^*_{mf} is the mean-field interference at the equilibrium, by assuming that the interfering IoT devices use their optimal power allocation strategy and m is a solution of

$$\begin{cases} \partial_t m(t,e) - \partial_e\big(P(t,e)m(t,e)\big) = 0, \\ m(0,.) = m_0. \end{cases} \tag{22}$$

Since F is convex in P, the mean-field optimal control is a convex optimization problem. Therefore, the first-order optimality conditions are necessary and sufficient for the mean-field equilibrium.

3.3.1. First-Order Optimality Conditions:

The first-order optimality conditions of the mean-field optimal control problem are derived using the adjoint method. Note that even though this approach is used formally in the following, it can be made rigorous. We refer the interested reader to [50] for a rigorous derivation of these first-order optimality conditions.
Let's start by defining the Lagrangian of the minimization problem (21) under the constraint (22) as

$$\mathcal{L}(P,m,\mu) = U_{mf}(P, I^*_{mf}, p_s) \quad - \int_0^{E_{max}}\int_0^{T_f} \mu(t,e)\left(\partial_t m(t,e) - \partial_e\big(P(t,e)m(t,e)\big)\right)\,dt\,de, \tag{23}$$

where $\mu(t,e)$ represent the Lagrange multiplier.
The minimization problem (21) can be rewritten as a saddle-point problem:

$$\inf_{(P,m)}\sup_{\mu} \mathcal{L}(P,m,\mu). \tag{24}$$

By using the integration by parts, the first-order conditions characterizing the saddle-point (P^*, m^*, μ^*) of $\mathcal{L}$ are expressed as (22) together with:

$$\partial_P F_{mf} - \partial_e \mu^* = 0, \tag{25}$$
$$\partial_t \mu^* - P^*\partial_e\mu^* + F_{mf} = 0, \tag{26}$$
$$\mu^*(T_f, .) = 0.. \tag{27}$$

Note that the equation (26) reflects the adjoint equation of (22), popularly known as the Hamilton-Jacobi-Bellman equation in mean-field game theory.
Finally, the mean-field equilibrium can be obtained as the solution of the following mean-field system:

$$\begin{cases} \partial_t m - \partial_e(Pm) = 0, \quad m(0,.) = m_0, \\ \partial_t\mu^* - P^*\partial_e\mu^* + F_{mf} = 0, \quad \mu^*(T_f,.) = 0, \\ \partial_P F_{mf} - \partial_e\mu^* = 0, \end{cases} \tag{28}$$

which consists of two coupled partial differential equations, one evolving forward in time (the Fokker-Planck Kolmogorov) and the other one evolving backward in time (the Hamilton-Jacobi-Bellman equation).

3.3.2. The Algorithm

The mean-field system (28) is solved iteratively until the convergence point is reached to achieve the mean-field equilibrium. We employ a successive sweep method, which entails generating a series of nominal solutions $P_0, P_1, \dots, P_k, \dots$ that converges to the optimal power allocation strategy P^*. This iterative approach, which has proven to be effective in [51], is summarized in algorithm 1 in our context. Moreover, a gradient-based implementation of this approach can be found in [52]. Finally, we refer the reader to [53] for a review of several aspects of numerical approaches for mean-field control problems.

Algorithm 1: Mean-Field Equilibrium

Initialization:

Generate initial transmit power P_0 ;

Learning pattern:

Find m using (22) with initial condition m_0 ;

Find p_s and π_a by solving algorithm 2 ;

Estimate interference I_{mf} using (16);

Find μ using (26) with final condition (27);

Update transmit power P using (25);

Repeat until convergence : go to step 2;

4. Grant-Free Markov Chain Model

In this section, we present a discrete-time Markov chain to derive a closed form for the probability of having at least one packet in an IoT device's queue, which implies the probability of attempting uplink transmissions. To determine this probability analytically, we must first acquire the transmission success probability p_s, which is defined as the probability that a packet is successfully transferred when an IoT device executes an uplink transmission.

It is worth mentioning that in this section, we will assume that IoT devices use their optimal power allocation strategy.

In our Markov chain model, each state represents the queue length of a generic IoT device, where the queue length implies the number of packets in the queue. The state space S can be defined as

$$S = \{0, 1, 2, \dots, M\}, \tag{29}$$

where M represents the queue size. Let's $\pi_i(n)$ be the state probability that the queue length equals i at time $n \in \{0, T_f, 2T_f, \dots\}$. Thus, the distribution of the state probability at time n, $\boldsymbol{\pi}(n)$, can be denoted as

$$\boldsymbol{\pi}(n) = \left[\pi_0(n), \pi_1(n), \dots, \pi_M(n)\right]. \tag{30}$$

The state transition probability from state j to state k, denoted as $q_{j,k}$, is given in (31).

4.1. Packet Transmission Success Probability

The transmission success probability at a generic BS is used to estimate the successful transmission probabilities of all IoT devices in the network. This means that such probabilities are independent of location and uncorrelated across time frames. Exploiting this approximation and accounting for the mean-field interference, the transmission success probability is characterized by the following proposition:

Proposition 2. *The transmission success probability of a generic IoT device whose generic BS is at the origin is*

$$p_s = \frac{\pi\lambda_s}{T_f}\sum_{j=0}^{J}\mathbb{P}[N_a = j]\times \int_0^{T_f}\int_0^{E_{max}}\left[\int_0^{\infty} e^{-ar^{\frac{\alpha}{2}}} e^{-br} dr\right] m^*(t,e)\, de\, dt, \tag{32}$$

where

$$\begin{cases} a = \dfrac{\theta(\sigma_0 + I^*_{mf}(t))}{P^*(t,e)}, \\ b = \pi\lambda_s. \end{cases} \tag{33}$$

Under urban areas where $\alpha \simeq 4$, we have

$$p_s = \frac{\pi\lambda_s}{T_f}\sum_{j=0}^{J}\mathbb{P}[N_a = j]\int_0^{T_f}\int_0^{E_{max}} g(a,b) m^*\, de\, dt, \tag{34}$$

where

$$g(a,b) = \sqrt{\frac{\pi}{a}}\exp(\frac{b^2}{4a})Q\left(\frac{b}{\sqrt{2a}}\right), \tag{35}$$

with

$$Q(x) = \frac{1}{\sqrt{2\pi}}\int_x^{\infty} e^{-\frac{u^2}{2}}\, du. \tag{36}$$

The Q function is the tail distribution of the standard normal distribution.

Proof. The proof is given in Appendix A.2.

$$q_{j,k} = \begin{cases} 1-p_a, & j=k=0 \\ p_a, & j=0, \quad k=1 \\ (1-p_a)p_b + (1-p_a)(1-p_b)(1-p_s) + p_a(1-p_b)p_s, & 1 \le j \le M-1, \quad k=j \\ 1-(1-p_a)(1-p_b)p_s, & j=k=M \\ p_a(1-p_b)(1-p_s) + p_a p_b & 1 \le j \le M-1, \quad k=j+1 \\ (1-p_a)(1-p_b)p_s, & 1 \le j \le M, \quad k=j-1 \\ 0, & \text{Otherwise.} \end{cases} \tag{31}$$

4.2. Steady-State Analysis

The steady-state distribution $\boldsymbol{\pi}$ for the M state Markov chain with transition matrix [K], given by using $q_{i,j}$ as the i_{th} row and j_{th} column element, is a row vector that satisfies

$$\boldsymbol{\pi} = \boldsymbol{\pi}[\mathrm{K}], \quad \text{where} \quad \langle \boldsymbol{\pi}, \mathbf{1} \rangle = 1 \quad \text{and} \quad \pi_i \ge 0. \tag{37}$$

Thus, the steady-state probabilities can be expressed as

$$\pi_0 = \pi_0 q_{0,0} + \pi_1 q_{1,0}, \tag{38}$$

$$\pi_i = \pi_{i-1} q_{i-1,i} + \pi_i q_{i,i} + \pi_{i+1} q_{i+1,i}, \quad i \in [1, M-1], \tag{39}$$

and

$$\pi_M = \pi_{M-1} q_{M-1,M} + \pi_M q_{M,M}. \tag{40}$$

Thus with above equations, we have

$$\pi_i = \begin{cases} \pi_0, & i=0, \\ \pi_0 \prod_{j=0}^{i-1} \left(\frac{q_{j,j+1}}{q_{j+1,j}} \right), & i \in [1, M]. \end{cases} \tag{41}$$

By using the normalization condition $\sum_i \pi_i = 1$, π_0 can be expressed as

$$\pi_0 = \left(1 + \sum_{i=1}^{M} \prod_{j=0}^{i-1} bigg(\frac{q_{j,j+1}}{q_{j+1,j}} \right) \right)^{-1}. \tag{42}$$

Therefore, the probability that an IoT device is active, i.e., there exist at least a packet in its queue, is given by

$$\pi_a = 1 - \pi_0 = 1 - \left(1 + \sum_{i=1}^{M} \prod_{j=0}^{i-1} \left(\frac{q_{j,j+1}}{q_{j+1,j}} \right) \right)^{-1}. \tag{43}$$

Note that the equations (32) and (43) form a non-linear system given $\boldsymbol{P}^*$ and m^*, which means that there is no closed-form solution that can be directly calculated. Therefore, π_a and p_s must be computed numerically. The algorithm 2 summarizes the numerical approach. The convergence of the algorithm 2

Algorithm 2: Learning p_s and π_a

Initialization:
1 Generate initial success probability p_s ;
2 Calculate π_a using (43) ;

Learning pattern:
3 Update p_s using (32);
4 Update π_a using (43) ;
5 Repeat until convergence : go to step 3;

is guaranteed due to the uniqueness of steady-state probabilities. In other words, given a fixed set of system parameters, the steady-state probabilities of the Markov chain are unique and can be obtained through numerical methods. Our iterative approach is based on updating the transmission success probability and the probability that an IoT device is active in each iteration until convergence is achieved.

4.3. Performance Metrics

By solving algorithm 1, we will obtain the optimal power allocation strategy as well as the Markov chain steady-state probabilities. As a result, we can now exploit them to estimate the average steady-state performance of grant-free access in terms of throughput, queue size, number of transmissions, and delay.
Note that, because of the Bernoulli arrival process, the packet generation is a geometric inter-arrival process with parameter p_a, i.e., the interval between two consecutive packet arrivals is a geometric random variable. As a result, the Geo/Geo/1/M queue can be used to represent the discrete-time queuing system of a generic IoT device. More precisely, since the success probability p_s

is uncorrelated across time frames, the service time (in number of frames) is also a geometric random variable with the parameter $(1 - p_b)p_s$.

- **Average throughput rate (service rate):** The average throughput rate, denoted as T_h, experienced by a generic IoT device writes

$$T_h = (1 - p_b)p_s. \tag{44}$$

It should be noted that access barring can affect the average throughput rate. More precisely, for a given p_b, the system can operate in either a saturated or unsaturated state. When $p_a > (1 - p_b)p_s$, the system is saturated, which means that all IoT devices have at least one packet to transmit. In contrast, when $p_a < (1 - p_b)p_s$, the system works in an unsaturated state.

- **Average number of transmissions (service time):** Let N_t represent the number of transmission attempts before a generic IoT device's packet is successfully transmitted, which follows a geometric distribution with parameter T_h, and its probability mass function can be written for $k \in \{1, 2, \dots\}$, as

$$f_{N_t}(k) = \left(1 - T_h\right)^{k-1} T_h. \tag{45}$$

Thus, the average number of transmissions per packet is given by:

$$\mathbb{E}[N_t] = \frac{1}{T_h}. \tag{46}$$

- **Average queue size:** At steady state, the average queue size of a generic IoT device can be estimated by

$$Q = \sum_{k=1}^{M} k\pi_k. \tag{47}$$

- **Average delay:** Let D denote the average delay experienced by a given packet at a generic IoT device, i.e., the average number of frames that a packet spent in the queue until successful transmission, which may be represented as

$$D = \underbrace{Q\mathbb{E}[N_t]}_{\text{queuing delay}} + \underbrace{\mathbb{E}[N_t]}_{\text{transmission delay}}. \tag{48}$$

It should be emphasized that when the system is saturated, the average delay increases dramatically.

5. Numerical Analysis

In this section, we offer some explanations below on how to numerically solve the algorithm 1 using a finite difference method and we present numerical results.

Table 1
Parameters for Numerical Results

Parameter	Values	Description
λ_s	1,5,10,20 BS/km^2	BS density
λ_u	3000 IoT/km^2	IoT density
p_b	0.1	Barring probability
p_a	1-60 packet/hour	Arrival rate
θ	10	SINR threshold
J	1,3,5,7	MPR capability
L	30	Number of channels
M	10	The queue size
P_{max}	0.025 W	Maximum power
T_f	10 ms	Frame duration
E_{max}	0.1 mJ	Maximum energy
σ_0	-200 dBm	Noise power
α	4	Path-loss exponent

5.1. Finite Difference Method

In order to numerically solve our algorithm, we consider a discretized grid within $[0, T_f] \times [0, E_{max}]$. Let us consider two positive integers, X and Y. We define the time and space steps by $\delta t = T_f / X$, $\delta E = E_{max}/Y$, and for $n = 0, \dots, X$, $i = 0, \dots, Y$, we denote f_i^n the numerical approximations of $f(n\delta t, i\delta E)$ for any function f. The FPK equation (22) is computed iteratively using a upwind-type finite difference scheme by:

$$m_i^{n+1} = m_i^n + \frac{\delta t}{\delta E}\left(P_{i+1}^n m_{i+1}^n - P_i^n m_i^n\right). \tag{49}$$

Moreover, for an arbitrary point (n, i), the optimality conditions (25), (26) are discretized as follows:

$$\frac{\partial F_i^n}{\partial P_i^n} - \frac{\left(\mu_i^n - \mu_{i-1}^n\right)}{\delta E} = 0, \tag{50}$$

$$\mu_i^{n-1} = \mu_i^n - \frac{\delta t}{\delta E} P_i^n \left(\mu_i^n - \mu_{i-1}^n\right) + F_i^n \delta t, \tag{51}$$

where

$$F_i^n = (1 - p_s)P_i^n - p_s \log_2\left(1 + \frac{P_i^n (2\sqrt{\lambda_s})^\alpha}{\sigma_0 + I_{mf}(t)}\right). \tag{52}$$

Figure 1: Optimal Power Allocation Strategies and transmission success probability for different BS densities with $p_a = 1$ packet / 5 min and $J = 3$.

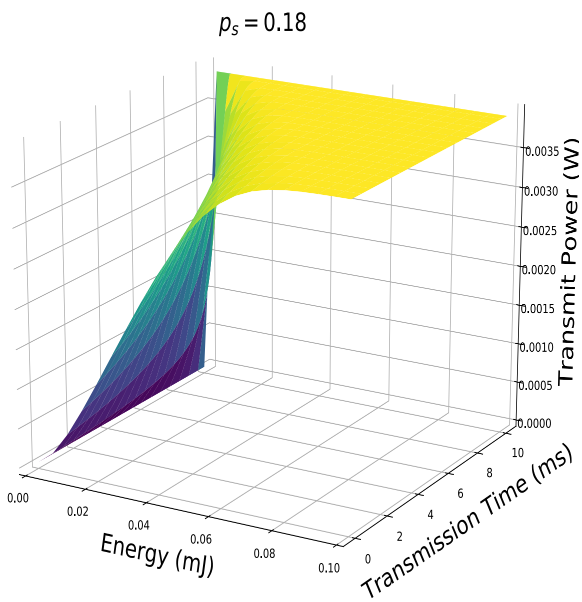

(a) $\lambda_s = 1$ BS / km^2

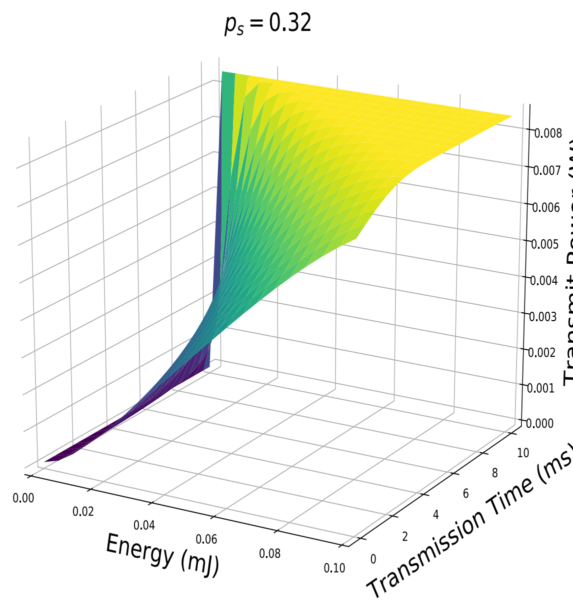

(b) $\lambda_s = 5$ BS / km^2

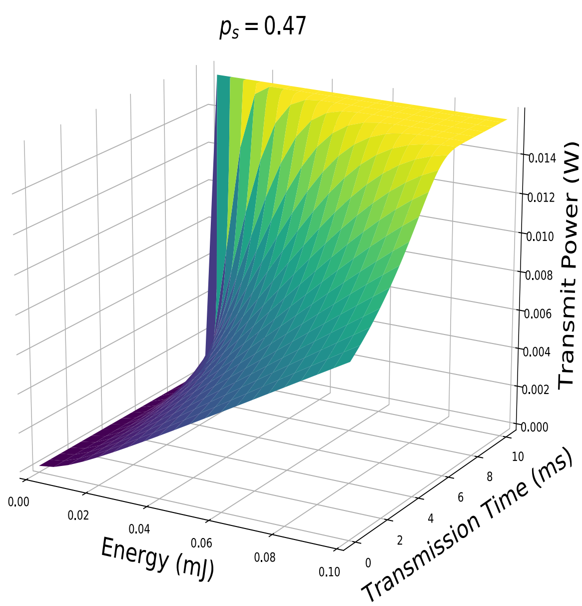

(c) $\lambda_s = 10$ BS / km^2

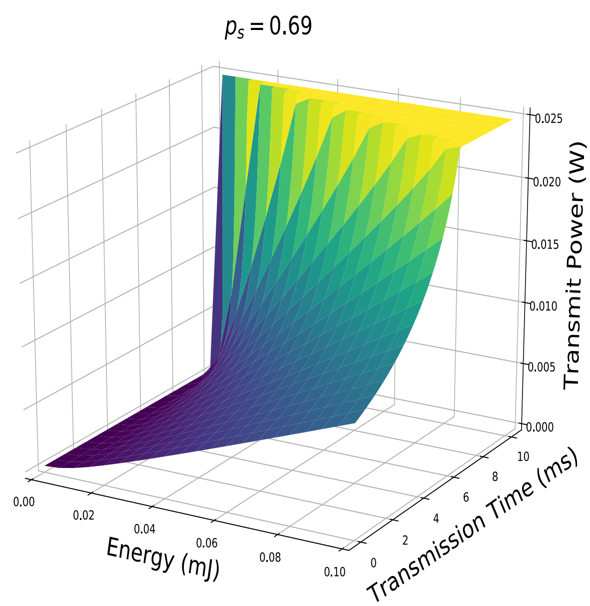

(d) $\lambda_s = 20$ BS / km^2

5.2. Numerical Results

We present numerical results on the performance of the algorithm 1. For all simulations, we choose $X = 100$ and $Y = 30$ to form a discretized space $X \times Y$, and we consider a uniform initial energy distribution m_0. Table 1 shows the typical values of parameters used for numerical results.

Optimal Power Allocation Strategy: The Figure 1 shows the optimal power allocation strategy and the transmission success probability for different BS densities. In this simulation, we set the arrival rate p_a to 1 packet / 5 min and the MPR capability J to 3. The IoT devices can adjust their transmit power based on their available energy at any given time. As the network becomes denser, both the transmission

Figure 2: mean-field at equilibrium for different BS densities with $p_a = 1$ packet / 5 min and $J = 3$.

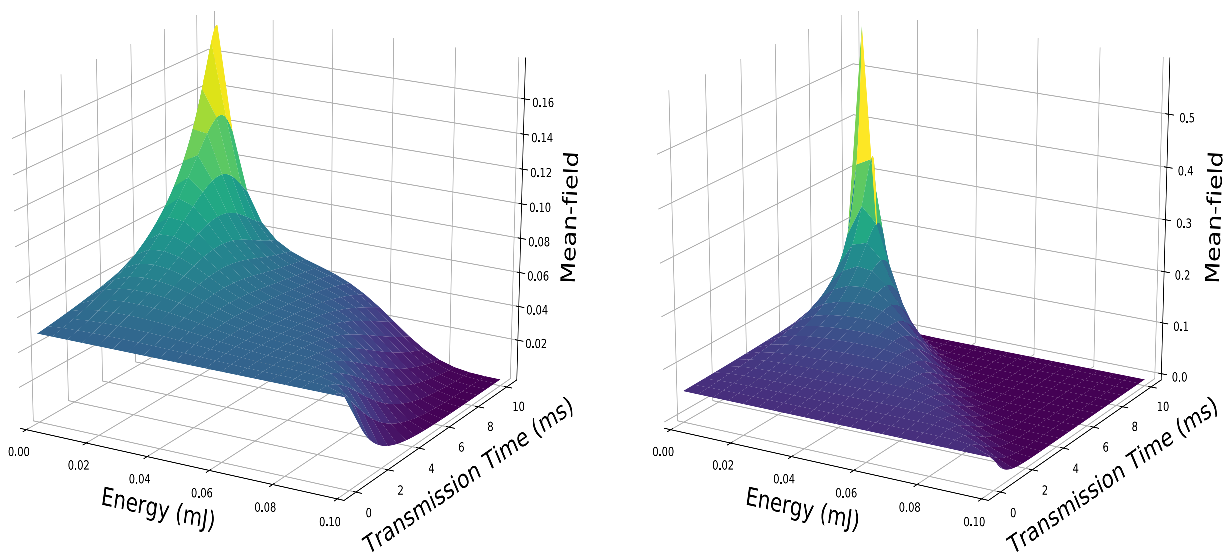

(a) $\lambda_s = 1$ BS / km^2 (b) $\lambda_s = 20$ BS / km^2

Figure 3: Cross-section of the mean-field at equilibrium for different BS densities and energy levels with $p_a = 1$ packet / 5 min and $J = 3$.

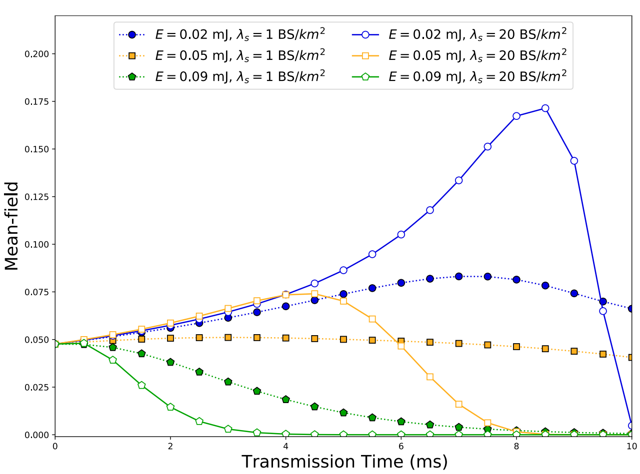

success probability and the number of points for which $P^* = P_{max}$ increase. It is worth noting that at the end of transmission, IoT devices with lower energy budgets empty their batteries, lowering the average network interference. As a result, the remaining IoT devices strategically boost their transmission power to maximize throughput.

Evolution of Energy Distribution: The mean-field at equilibrium is shown in Figure 2 for two BS densities. The Figure 3 illustrates a cross-section of this mean-field at fixed energy levels. Both figures illustrate the temporal evolution of the energy distribution. As stated before, a uniform initial energy distribution m_0 is considered. It can be seen that the fraction of IoT devices with higher energy reduces over time, especially in the case of a dense network. This is because IoT devices increase their transmit power since they can achieve a better success probability. Meanwhile, when λ_s is set to 1 BS/km^2, approximately 13% of the IoT devices use up their whole energy budget during transmission. It is noteworthy that transmitting at maximum power in less dense networks is not only inefficient but also leads to energy waste, offering minimal improvement in success probability.

Impact of Network Densification and MPR Capability on Average Delay: The benefits of increasing base station density and improving multi-packet reception capability are highlighted in Figure 4 and Figure 5 by investigating the average delay. More precisely, Figure 4 illustrates the average delay in number of frames as a function of BS densities for various arrival rates. The reduction in average delay with increasing BS density aligns with expectations, as a higher density shortens the distance between IoT devices and their serving BSs, enhancing reliability. This insight gains

Figure 4: Average delay as a function of BS densities for various arrival rates with $J = 3$.

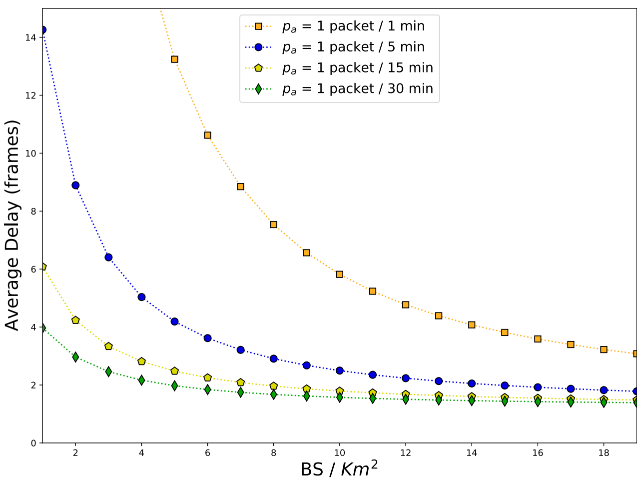

Figure 5: Average delay as a function of BS densities for various multi-packet reception capabilities with $p_a = 1$ packet / 1 min.

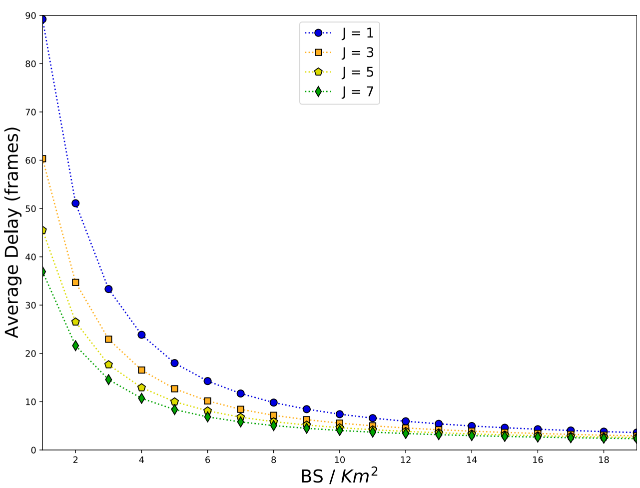

prominence in the context of grant-free communication, where efficient transmission is critical due to the absence of handshaking procedures. The figure further demonstrates that as the BS density grows, the difference in the average delay between different arrival rate scenarios narrows. This is because a higher density of BSs can handle more traffic and reduce network congestion. Thus, the delay of an IoT device is reduced, regardless of the arrival rate.
Moreover, Figure 5 shows the average delay as a function of BS densities for various multi-packet reception capabilities. It shows that as the MPR capability improves, the average delay reduces. However, the figure clearly demonstrates that the advantage of MPR capability fades as the network becomes denser. This is due to the fact that the number of resources, such as channels and MPR, increases with the number of BSs. Hence, the additional resources have little or no effect on reducing the average delay. Thus, This insight highlight the need for a balanced approach in optimizing network resources.

Impact of IoT Density on Average Delay: The influence of IoT density on average delay is highlighted in Figure 6 and Figure 7. In Figure 6, the average delay is illustrated as a function of IoT density for different arrival rates. The Figure 7, on the other hand, shows the average delay as a function of IoT density for various BS densities. Both figures indicate that as the IoT density increases, the average delay also increases. This is because an increase in IoT density leads to more IoT devices contending for the same resources, resulting in congestion and increased delay. However, in low-traffic conditions, the average delay remains acceptable even as the IoT density increases. Moreover, the Figure 7 underscores the importance of carefully managing network densification to enhance reliability and minimize delays as IoT density increases.

Impact of IoT Density and Arrival Rate on Success Probability: Finally, the influence of IoT density and arrival rate on the success transmission probability is highlighted in Figure 8 and Figure 9. It is worth noting that the success probability in these figures represents the probability of successfully transmitting a packet in a single frame. This probability can be compared to the success probability of the slotted Aloha protocol, which is approximately 18% for a single device. The Figure 8 shows the success probability as a function of the arrival rates for different MPR capabilities and BS densities. It suggests that in low-traffic scenarios, maintaining a high success probability is achievable without extensive network densification or advanced MPR capability. However, under high-traffic conditions, these enhancements prove beneficial. On the other hand, Figure 9 illustrates the success probability as a function of IoT densities for different arrival rates and BS densities. It emphasizes the inverse relationship between IoT density and success probability. It also indicates, reinforcing prior findings, that network densification improves success probability, particularly in massive IoT environments.

6. Conclusion

The paper explores grant-free access with multi-packet reception capabilities, focusing on low-end IoT

Figure 6: Average delay as a function of IoT device densities for various arrival rates with $\lambda_s = 10$ BS / km^2 and $J = 3$.

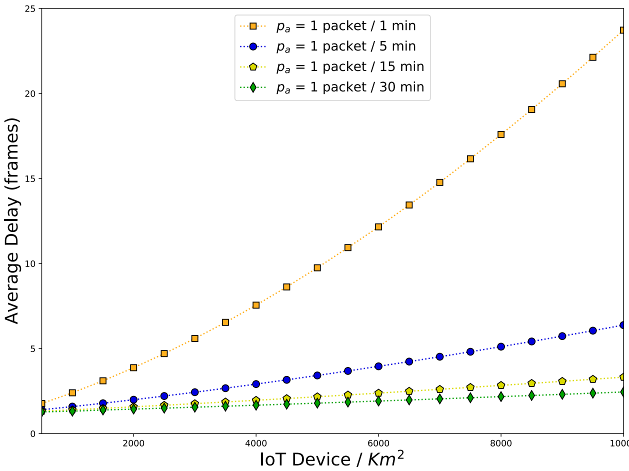

Figure 7: Average delay as a function of IoT device densities for various BS densities with $p_a = 1$ packet / 1 min and $J = 3$.

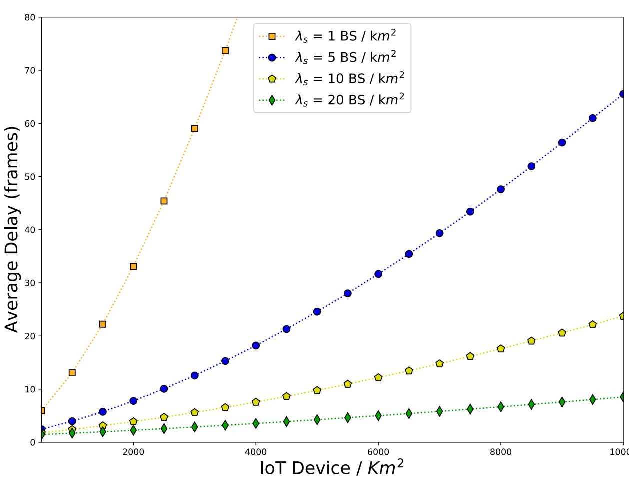

Figure 8: Success probability as a function of arrival rates for various multi-packet reception capabilities and BS densities.

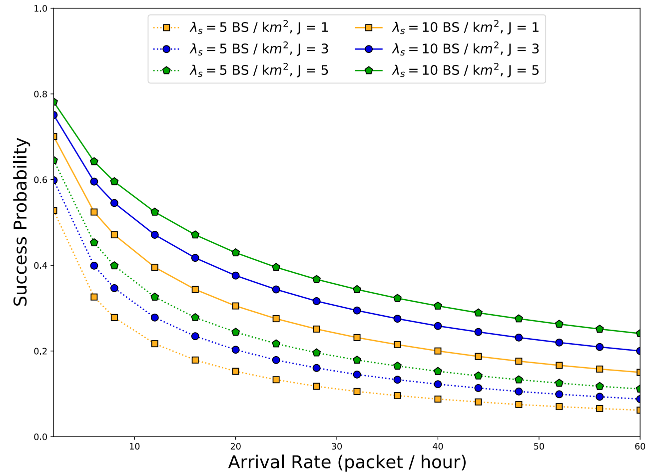

Figure 9: Success probability as a function of IoT device densities for various arrival rates and BS densities with $J = 3$.

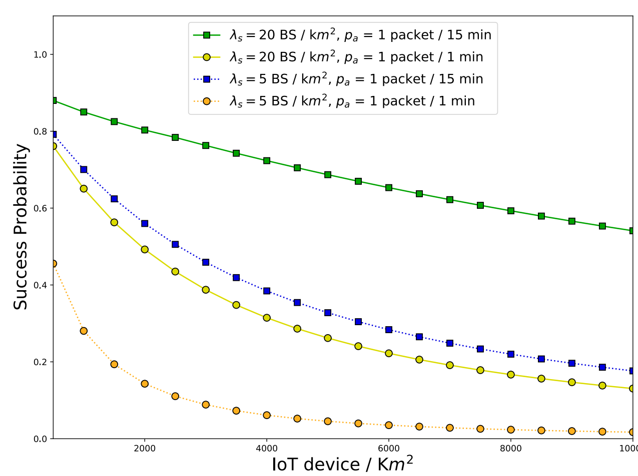

devices characterized by small data sizes, sporadic activity, and strict energy constraints. The main contribution lies in introducing a traffic-aware distributed power allocation algorithm for grant-free massive IoT networks. The algorithm ensures that IoT devices meet their throughput expectations while minimizing energy usage. Thus, each IoT device autonomously computes its optimal power allocation strategy based only on its individual energy level and the initial energy distribution, considering the given arrival rate. Our approach leverages the mean-field framework to capture population behavior and employs the Markov chain framework to derive the transmission success probability. The numerical results illustrate the optimal power allocation strategy and examine how network densification, MPR capability, IoT density, and arrival rate collectively impact average delay and transmission success probability. A noteworthy aspect of the proposed algorithm is its offline execution capability without the need for information exchange with the base station, a significant advantage in grant-free networks. However, a limitation of the current model is the assumption of a uniform arrival rate for all IoT devices, diverging from the heterogeneous traffic patterns observed in practical scenarios. To address this, we are particularly willing to examine various classes of IoT devices, each characterized by its own unique traffic profile. Such an investigation aims to offer a more realistic representation of IoT traffic dynamics, thereby augmenting the algorithm's practical applicability.

A. Appendix

A.1. Proof of proposition 1

Without loss of generality, we derive the finite mean-field interference for an IoT device i whose BS is at the origin.
The mean-field interference in C_R for a given time instant $t \in [0, T_f]$ is expressed as:

$$I_{i,mf}(t) = \mathbb{E}\left[\sum_{j=1, j\neq i}^{|\mathcal{N}_R|} P(t, E_j(t)) H_{i,j}(t) D_{i,j}(r)\right]. \quad (53)$$

It is worth noting that, in the mean-field regime, the IoT devices become essentially indistinguishable, and a single IoT device has a negligible effect on the overall mass behavior. Thus, we can focus on a generic IoT device while dropping the index i from (53). Since the transmit power of a generic IoT device is independent of the point process and h is exponentially distributed with unity mean, the previous formula writes

$$I_{mf}(t) = \mathbb{E}\left[P(t, E)\right] \mathbb{E}_{\phi_a}\left[\sum_{j=1, j\neq i}^{|\mathcal{N}_R|} D(r)\right], \quad (54)$$

where

$$\mathbb{E}[P(t, E)] = \int_0^{E_{max}} P(t, e) m(t, e)\, de. \quad (55)$$

Then, by using Campbell's formula, we write:

$$\mathbb{E}_{\phi_a}\left[\sum_{j=1, j\neq i}^{|\mathcal{N}_R|} r^{-\alpha}\right] = 2\pi\lambda_u \frac{(1-p_b)\pi_a}{L} \int_0^R D(r) r dr. \quad (56)$$

Since the received power cannot be greater than the transmitted power, the path-loss is assumed to be 1 when $r < 1$. Then, we have

$$\begin{aligned} \int_0^R D(r) r dr &= \int_0^1 r dr + \int_1^R r^{1-\alpha} dr \\ &= \frac{1}{2} + \frac{1 - R^{\alpha-2}}{2-\alpha}. \end{aligned} \quad (57)$$

Finally, considering a large-scale network and taking $R \to \infty$ concludes the proof.

A.2. Proof of proposition 2

The transmission success probability is given by

$$p_s = \underbrace{\sum_{j=0}^{J} \mathbb{P}[N_a = j]}_{\text{probability of no packet collision}} \times p_\theta \quad (58)$$

where p_θ is the probability that the SINR of a generic IoT device, whose generic BS is at the origin , is greater than θ over a given frame with duration T_f expressed as

$$\begin{aligned} p_\theta &= \frac{1}{T_f} \int_0^{T_f} \mathbb{P}\left[\frac{P^*(t,e) H r^{-\alpha}}{\sigma_0 + I} \geq \theta\right] dt \\ &\approx \frac{1}{T_f} \int_0^{T_f} \mathbb{P}\left[\frac{P^*(t,e) H}{r}^{-\alpha} \sigma_0 + I^*_{mf} \geq \theta\right] dt. \end{aligned} \quad (59)$$

Conditioning on the energy and the distance from a generic IoT device to its nearest BS, we get

$$\begin{aligned} p_\theta &= \frac{1}{T_f} \int_0^{T_f} \mathbb{E}\left[\mathbb{P}\left[\frac{P^*(t,e) H r^{-\alpha}}{\sigma_0 + I^*_{mf}} \geq \theta \middle| r, e\right]\right] dt \\ &= \frac{1}{T_f} \int_0^{T_f} \int_0^{E_{max}} \left[\int_0^{\infty} \mathbb{P}\left[H \geq a r^\alpha\right] f_r dr\right] m^* \, de\, dt, \end{aligned} \quad (60)$$

where $a = \theta(\sigma_0 + I^*_{mf}(t))/P^*(t, e)$.
Using the fact that $H \sim \exp(1)$, we have

$$\mathbb{P}\left[H \geq a r^\alpha\right] = e^{-a r^\alpha}. \quad (61)$$

Thus, replacing the probability density function f_r by its expression given in equation (2), yields

$$p_\theta = \frac{2\pi\lambda_s}{T_f} \int_0^{T_f} \int_0^{E_{max}} \left[\int_0^{\infty} e^{-a r^\alpha} e^{-b r^2} r dr\right] m^*(t, e)\, de\, dt. \quad (62)$$

where $b = \pi\lambda_s$.
Using the substitution $s = r^2$ in the inside integral of (62) and combining with (58), we obtain the result.
Finally, in the special case where $\alpha = 4$, we have the following result:

$$\int_0^{\infty} e^{-a r^2} e^{-b r} dr = \sqrt{\frac{\pi}{a}} \exp\left(\frac{b^2}{4a}\right) Q\left(\frac{b}{\sqrt{2a}}\right), \quad (63)$$

where

$$Q(x) = \frac{1}{\sqrt{2\pi}} \int_{x}^{\infty} e^{-\frac{u^2}{2}} du. \tag{64}$$

This concludes the proof.

References

[1] Krishna Kumar, Aman Kumar, Narendra Kumar, Mazin Abed Mohammed, Alaa S. Al-Waisy, Mustafa Musa Jaber, Rachna Shah, Mohammed Nasser Al-Andoli, and Varun Menon. Dimensions of internet of things: Technological taxonomy architecture applications and open challenges—a systematic review. *Wirel. Commun. Mob. Comput.*, 2022, jan 2022.

[2] Gaetanino Paolone, Danilo Iachetti, Romolo Paesani, Francesco Pilotti, Martina Marinelli, and Paolino Di Felice. A holistic overview of the internet of things ecosystem. *IoT*, 3(4):398–434, 2022.

[3] Moongi Choi, Sung-Jin Cho, and Chul Sue Hwang. Relieving bottlenecks during evacuations using iot devices and agent-based simulation. *Sustainability*, 13(16), 2021.

[4] Neha Koul, Neerendra Kumar, Aqsa Sayeed, Chaman Verma, and Maria Simona Raboaca. Data exchange techniques for internet of robotic things: Recent developments. *IEEE Access*, 10:102087–102106, 2022.

[5] Muhammad Basit Shahab, Rana Abbas, Mahyar Shirvanimoghaddam, and Sarah J. Johnson. Grant-free non-orthogonal multiple access for iot: A survey. *IEEE Communications Surveys and Tutorials*, 22(3):1805–1838, 2020.

[6] Fengming Cao and Zhong Fan. Cellular m2m network access congestion: Performance analysis and solutions. In *2013 IEEE 9th International Conference on Wireless and Mobile Computing, Networking and Communications (WiMob)*, pages 39–44, 2013.

[7] Amin Azari, Petar Popovski, Guowang Miao, and Cedomir Stefanovic. Grant-free radio access for short-packet communications over 5g networks. In *GLOBECOM 2017 - 2017 IEEE Global Communications Conference*, pages 1–7, 2017.

[8] Mao Yang, Bo Li, Zhicheng Bai, and Zhongjiang Yan. Sgma: Semi-granted multiple access for non-orthogonal multiple access (noma) in 5g networking. *Journal of Network and Computer Applications*, 112:115–125, 2018.

[9] Jinho Choi, Jie Ding, Ngoc-Phuc Le, and Zhiguo Ding. Grant-free random access in machine-type communication: Approaches and challenges. *IEEE Wireless Communications*, 29(1):151–158, 2022.

[10] Fei Gu, Jianwei Niu, Landu Jiang, Xue Liu, and Mohammed Atiquzzaman. Survey of the low power wide area network technologies. *Journal of Network and Computer Applications*, 149:102459, 2020.

[11] Imane Cheikh, Rachid Aouami, Essaid Sabir, Mohamed Sadik, and Sébastien Roy. Multi-layered energy efficiency in lora-wan networks: A tutorial. *IEEE Access*, 10:9198–9231, 2022.

[12] Andrea Munari. Modern random access: An age of information perspective on irregular repetition slotted aloha. *IEEE Transactions on Communications*, 69(6):3572–3585, 2021.

[13] Ruizhe Qi, Xuefen Chi, Linlin Zhao, and Wanting Yang. Martingales-based aloha-type grant-free access algorithms for multi-channel networks with mmtc/urllc terminals co-existence. *IEEE Access*, 8:37608–37620, 2020.

[14] Sotiris A. Tegos, Panagiotis D. Diamantoulakis, Athanasios S. Lioumpas, Panagiotis G. Sarigiannidis, and George K. Karagiannidis. Slotted aloha with noma for the next generation iot. *IEEE Transactions on Communications*, 68(10):6289–6301, 2020.

[15] Fan Wu, Guobao Sun, and Guihai Chen. On multipacket reception based neighbor discovery in low-duty-cycle wireless sensor networks. *Computer Communications*, 75:71–80, 2016.

[16] Arun George and T.G. Venkatesh. Multi-packet reception dynamic frame-slotted aloha for iot: Design and analysis. *Internet of Things*, 11:100256, 2020.

[17] Hamid Tahaei, Firdaus Afifi, Adeleh Asemi, Faiz Zaki, and Nor Badrul Anuar. The rise of traffic classification in iot networks: A survey. *Journal of Network and Computer Applications*, 154:102538, 2020.

[18] Zheng Yang, Peng Xu, Jamal Ahmed Hussein, Yi Wu, Zhiguo Ding, and Pingzhi Fan. Adaptive power allocation for uplink non-orthogonal multiple access with semi-grant-free transmission. *IEEE Wireless Communications Letters*, 9(10):1725–1729, 2020.

[19] Renato Abreu, Thomas Jacobsen, Gilberto Berardinelli, Klaus Pedersen, István Z. Kovács, and Preben Mogensen. Power control optimization for uplink grant-free urllc. In *2018 IEEE Wireless Communications and Networking Conference (WCNC)*, pages 1–6, 2018.

[20] Xin Jian, Langyun Wu, Keping Yu, Moayad Aloqaily, and Jalel Ben-Othman. Energy-efficient user association with load-balancing for cooperative iiot network within b5g era. *Journal of Network and Computer Applications*, 189:103110, 2021.

[21] Sana Benhamaid, Abdelmadjid Bouabdallah, and Hicham Lakhlef. Recent advances in energy management for green-iot: An up-to-date and comprehensive survey. *Journal of Network and Computer Applications*, 198:103257, 2022.

[22] Hesham ElSawy, Ahmed Sultan-Salem, Mohamed-Slim Alouini, and Moe Z. Win. Modeling and analysis of cellular networks using stochastic geometry: A tutorial. *IEEE Communications Surveys and Tutorials*, 19(1):167–203, 2017.

[23] Yassine Hmamouche, Mustapha Benjillali, Samir Saoudi, Halim Yanikomeroglu, and Marco Di Renzo. New trends in stochastic geometry for wireless networks: A tutorial and survey. *Proceedings of the IEEE*, 109(7):1200–1252, 2021.

[24] Qirui Liu, Rongke Liu, Yang Zhang, Yanli Yuan, Zijie Wang, Haolan Yang, Lin Ye, Mohsen Guizani, and John S. Thompson. Management of positioning functions in cellular networks for time-sensitive transportation applications. *IEEE Transactions on Intelligent Transportation Systems*, 24(11):13260–13275, 2023.

[25] A.B. MacKenzie and S.B. Wicker. Selfish users in aloha: a game-theoretic approach. In *IEEE 54th Vehicular Technology Conference. VTC Fall 2001. Proceedings (Cat. No.01CH37211)*, volume 3, pages 1354–1357 vol.3, 2001.

[26] Eitan Altman, Nicolas Bonneau, Merouane Debbah, and Giuseppe Caire. An evolutionary game perspective to aloha with power control. In ITC, editor, *ITC 19, 19th International Teletraffic Congress, August 29-September 2, 2005, Beijing, China*, Beijing, 2005.

[27] Essaid Sabir, Rachid El-Azouzi, and Yezekael Hayel. Hierarchy sustains partial cooperation and induces a braess-like paradox in slotted aloha-based networks. *Computer Communications*, 35(3):273–286, 2012.

[28] Lijun Chen, Steven H. Low, and John C. Doyle. Contention control: A game-theoretic approach. In *2007 46th IEEE Conference on Decision and Control*, pages 3428–3434, 2007.

[29] Rajni Gupta and Juhi Gupta. Future generation communications with game strategies: A comprehensive survey. *Computer Communications*, 192:1–32, 2022.

[30] Xiaoxia Zeng. Game theory-based energy efficiency optimization model for the internet of things. *Computer Communications*, 183:171–180, 2022.

[31] Leonardo Badia and Andrea Munari. A game theoretic approach to age of information in modern random access systems. In *2021 IEEE Globecom Workshops (GC Wkshps)*, pages 1–6, 2021.

[32] Ahmed Alioua, Roumayssa Hamiroune, Oumayma Amiri, Manel Khelifi, Sidi mohammed Senouci, Mikael Gidlund, and Sarder Fakhrul Abedin. Incentive mechanism for competitive edge caching in 5g-enabled internet of things. *Computer Networks*, 213:109096, 2022.

[33] Sami Nadif, Essaid Sabir, Halima Elbiaze, and Abdelkrim Haqiq. A hierarchical green mean-field power control with embb-mmtc coexistence in ultradense 5g. *To appear in the 20th International Symposium on Modeling and Optimization in Mobile, Ad Hoc, and Wireless Networks (WiOpt)*, 2022.

[34] Jean-Michel Lasry and Pierre-Louis Lions. Jeux à champ moyen. ii – horizon fini et contrôle optimal. *Comptes Rendus Mathematique*, 343(10):679–684, 2006.

[35] Olivier Guéant. A reference case for mean field games models. *Journal de Mathématiques Pures et Appliquées*, 92(3):276–294, 2009.

[36] Pierre Cardaliaguet and Alessio Porretta. *An Introduction to Mean Field Game Theory*, pages 1–158. Springer International Publishing, Cham, 2020.

[37] Diogo Gomes and Joao Saude. Mean field games models—a brief survey. *Dynamic Games and Applications*, 4, 06 2014.

[38] Minyi Huang, Roland Malhame, and Peter Caines. Large population stochastic dynamic games: Closed-loop mckean-vlasov systems and the nash certainty equivalence principle. *Commun. Inf. Syst.*, 6, 01 2006.

[39] Sami Nadif, Essaid Sabir, and Abdelkrim Haqiq. A mean-field framework for energy-efficient power control in massive iot environments. In *2019 IEEE 30th Annual International Symposium on Personal, Indoor and Mobile Radio Communications (PIMRC)*, pages 1–6, 2019.

[40] Dezhi Wang, Wei Wang, Zhaoyang Zhang, and Aiping Huang. Delay-optimal random access in large-scale energy harvesting iot networks based on mean field game. *China Communications*, 19(4):121–136, 2022.

[41] Sami Nadif, Essaid Sabir, Halima Elbiaze, and Abdelkrim Haqiq. Traffic-aware mean-field power allocation for ultra-dense nb-iot networks. *IEEE Internet of Things Journal*, pages 1–1, 2022.

[42] Hongliang Zhang, Yuhan Kang, Lingyang Song, Zhu Han, and H. Vincent Poor. Age of information minimization for grant-free non-orthogonal massive access using mean-field games. *IEEE Transactions on Communications*, 69(11):7806–7820, 2021.

[43] Wei-Chiang Wu. Identification of active users for grant-free massive connectivity in large scale antenna systems. *Journal of the Franklin Institute*, 358(16):8772–8785, 2021.

[44] Yi Zhong, Guoqiang Mao, Xiaohu Ge, and Fu-Chun Zheng. Spatio-temporal modeling for massive and sporadic access. *IEEE Journal on Selected Areas in Communications*, 39(3):638–651, 2021.

[45] Vijayalakshmi Chetlapalli, Himanshu Agrawal, K.S.S. Iyer, Mark A. Gregory, Vidyasagar Potdar, and Reza Nejabati. Performance evaluation of iot networks: A product density approach. *Computer Communications*, 186:65–79, 2022.

[46] Yan Liu, Yansha Deng, Maged Elkashlan, Arumugam Nallanathan, and George K. Karagiannidis. Analyzing grant-free access for urllc service. *IEEE Journal on Selected Areas in Communications*, 39(3):741–755, 2021.

[47] Mohammad Gharbieh, Hesham ElSawy, Mustafa Emara, Hong-Chuan Yang, and Mohamed-Slim Alouini. Grant-free opportunistic uplink transmission in wireless-powered iot: A spatio-temporal model. *IEEE Transactions on Communications*, 69(2):991–1006, 2021.

[48] Hesham ElSawy and Ekram Hossain. On cognitive small cells in two-tier heterogeneous networks. In *2013 11th International Symposium and Workshops on Modeling and Optimization in Mobile, Ad Hoc and Wireless Networks (WiOpt)*, pages 75–82, 2013.

[49] Gabriel Y. Weintraub, C. Lanier Benkard, and Benjamin Van Roy. Oblivious equilibrium: A mean field approximation for large-scale dynamic games. In *NIPS*, 2005.

[50] Giacomo Albi, Young-Pil Choi, Massimo Fornasier, and Dante Kalise. Mean field control hierarchy, 2016.

[51] E. Carlini and F. J. Silva. A fully discrete semi-lagrangian scheme for a first order mean field game problem. *SIAM Journal on Numerical Analysis*, 52(1):45–67, 2014.

[52] Martin Burger, Marco Di Francesco, Peter A. Markowich, and Marie-Therese Wolfram. Mean field games with nonlinear mobilities in pedestrian dynamics. *Discrete and Continuous Dynamical Systems - B*, 19(5):1311–1333, 2014.

[53] Mathieu Lauriere. Numerical methods for mean field games and mean field type control, 2021.

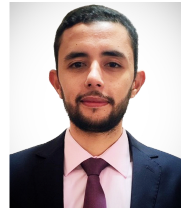

Sami Nadif (Student Member, IEEE) obtained his Master degree in applied mathematics and computation in 2017, from the Faculty of Science and Technology, Hassan First University of Settat, Morocco. Sami holds a part-time lecturer position at the Moroccan School of Engineering Sciences since 2020. He is currently pursuing his Ph.D. in the Department of Computing, Networks Mobility and Modeling at Hassan First University. His main research interests include self-organized networks, ubiquitous networks, the internet of things, game theory, and learning approaches for ultra-dense wireless networks.

Essaid Sabir (Senior Member, IEEE) received the B.Sc. degree and the M.Sc. degree in ECE from Mohammed V University of Rabat in 2004 and 2007 respectively, and the Ph.D. degree (Hons.) in networking and computer engineering from Avignon University, France, in 2010. He held a non-tenure-track Assistant Professor position at Avignon University, from 2009 to 2012. He has been a full Professor at Hassan II university of Casablanca until late 2022. Next, he joined the department of computer science, Université du Québec à Montréal as a professor until january 2024. Currently, he is a professor with the department of science and technology at TÉLUQ, University of Quebec. He is/was the main investigator of many research projects, and has been involved in several other (inter)national projects. His research interests include 5G/6G, IoT, ubiquitous networking, AI/ML, and networking games. His work has been awarded in many international venues. To bridge the gap between academia and industry, he founded the International Conference on Ubiquitous Networking (UNet) and co-founded the WINCOM conference series. He serves as an associate/guest editor for many journals. He organized numerous events and played executive roles for many major venues.

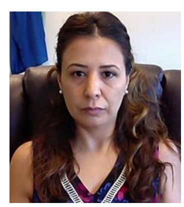

Halima Elbiaze (Senior Member, IEEE) received the B.Sc. degree in applied mathematics from Mohammed V University, Rabat, Morocco, in 1996, the M.Sc. degree in telecommunication systems from the Université de Versailles, Versailles, France, in 1998, and the Ph.D. degree in computer science from the Institut National des Télécommunications, Paris, France, in 2002. Since 2003, she has been with the Department of Computer Science, Université du Québec à Montréal, Montreal, QC, Canada, where she is currently an Associate Professor. She has authored or co-authored many journal and conference papers. Her current research interests include network performance evaluation, traffic engineering, and quality of service management in optical and wireless networks.

Abdelkrim Haqiq (Senior Member, IEEE) has a High Study Degree (Diplôme des Etudes Supérieures de troisième cycle) and a PhD (Docrotat d'état), both in modeling and performance evaluation of computer networks communications, from Mohammed V University of Rabat, Morocco. Since September 1995 he has been working as a Professor at the department of Applied Mathematics and Computer at the Faculty of Sciences and Techniques, Settat, Morocco. He is the Director of Computer, Networks, Mobility and Modeling laboratory (IR2M). He is also a member of Machine Intelligence Research Labs (MIR Labs), Washington-USA, and a member of the International Association of Engineers. He was a co-director of a NATO Multi-Year project entitled "Cyber-Security Analysis and Assurance using Cloud-Based Security Measurement system" (SPS-984425). His interests lie in the areas of modeling and performance evaluation of communication networks, mobile communications networks, cloud computing and security, emergent technologies, Markov Chains and queueing theory, Markov decision processes theory, and game theory. He has (co)authored more than 170 journal/conference papers. He serves as associate editor, editorial board member, international advisory board member, and editorial review board member of many international journals. He was a chair and a technical program committee chair/member of many international conferences. He was also a Guest Editor for many journals, books and conference proceedings.